Novel chloride-dependent acid loader in the guinea-pig ventricular myocyte: part of a dual acid-loading mechanism

Bing Sun, Chae Hun Leem and Richard D. Vaughan-Jones*

University Laboratory of Physiology, Parks Road, Oxford OX1 3PT, UK

1. The fall of intracellular pH (pH_i) following the reduction of extracellular pH (pH_o) was investigated in guinea-pig isolated ventricular myocytes using intracellular fluorescence measurements of carboxy-SNARF-1 (to monitor pH_i). Cell superfusates were buffered either with a 5% CO_2–HCO_3^- system or were nominally CO_2–HCO_3^- free.

2. Reduction of pH_o from 7·4 to 6·4 reversibly reduced pH_i by about 0·4 pH units, independent of the buffer system used.

3. In HCO_3^--free conditions, acid loading in low pH_o was not dependent on Na^+–H^+ exchange or on the presence of Na^+. It was unaffected by high-K^+ solution, by voltage-clamp depolarization, by various divalent cations (Zn^{2+}, Cd^{2+}, Ni^{2+} and Ba^{2+}) and by the organic Ca^{2+} channel blocker diltiazem, thus ruling out proton influx through H^+- or Ca^{2+}-conductance channels or influx via a K^+–H^+ exchanger. The fall also persisted in the presence of glycolytic inhibitors, or the lactate transport inhibitor, α-cyano-4-hydroxy cinnamate.

4. In HCO_3^--free conditions, acid loading in low pH_o was reversibly inhibited (by up to 85%) by Cl_o^- removal and was slowed by the stilbene drug DBDS (dibenzamidostilbene disulphonic acid). In contrast, the Cl^-–HCO_3^- exchange inhibitor DIDS (4,4′-diisothiocyanatostilbene-2,2′-disulphonic acid) had no inhibitory effect. Acid loading is therefore mediated by a novel Cl^--dependent, acid influx pathway.

5. After switching to CO_2–HCO_3^--buffered conditions, acid loading was doubled. It was still not inhibited by Na^+-free or high-K^+ solutions but was once again inhibited (by 78%) in Cl^--free solution. The HCO_3^--stimulated fraction of acid loading was inhibited by DIDS.

6. We propose a model of acid loading in the cardiomyocyte which consists of two parallel carriers. One is Cl^-–HCO_3^- exchange, while we suggest the other to be a novel Cl^-–OH^- exchanger (although we do not rule out the alternative configuration of H^+–Cl^- co-influx). The proposed dual acid-loading mechanism accounts for most of the sensitivity of pH_i to a fall of pH_o.

Intracellular pH is an important physiological modulator of cardiac contraction (see Orchard & Kentish, 1990 for review). This is largely because reducing pH_i reduces Ca^{2+} binding to troponin-C, thereby attenuating the force of contraction. Of the many conditions that can reduce pH_i in cardiac cells, a common one is a reduction of *extracellular* pH. Over the physiological range of pH, intracellular pH is related approximately linearly to pH_o, with a transfer function (slope of pH_i *vs.* pH_o) of 0·3–0·4 (Ellis & Thomas, 1976; Vaughan-Jones, 1986). Thus, because extracellular pH is an important modulator of pH_i in cardiac cells, it becomes an important modulator of contractility in the heart. The *mechanism*, however, whereby pH_i is linked to pH_o remains unknown (Sun & Vaughan-Jones, 1994). This is the case not only for cardiac cells, but also for many other cell types. In the present work, we have investigated the mechanism linking pH_i to pH_o in single enzymically isolated cardiomyocytes, while measuring pH_i using the pH-sensitive fluorophore, carboxy-SNARF-1. In particular, we have examined the mechanism responsible for intracellular acidosis in response to extracellular acidosis. Because pH_i is also sensitive to changes of P_{CO_2}, and because this latter effect is independent of pH_o (CO_2 is freely membrane permeant and its intracellular hydration generates H^+ ions), the present work was conducted either under conditions of *constant* external P_{CO_2} (5% CO_2) or in the nominal *absence* of CO_2 (by using air-equilibrated solutions, nominally free of CO_2).

* To whom correspondence should be addressed.

We identify two independent mechanisms that can import acid equivalents into the cardiac cell, and which play a roughly equal role in determining the sensitivity of cardiac pH_i to reduced pH_o. Preliminary accounts of some of this work have been published (Sun & Vaughan-Jones, 1994; Leem & Vaughan-Jones, 1995).

METHODS

Isolation of guinea-pig ventricular myocytes

The composition of solutions used for the isolation, and details of the procedure have been described previously (Lagadic-Gossmann, Buckler & Vaughan-Jones, 1992*a*). Briefly, single ventricular myocytes were isolated from 350–450 g albino guinea-pigs (killed by cervical dislocation) using a combination of enzymatic and mechanical dispersion (0·8 mg ml^{-1} collagenase, Type I or II, Worthington and 0·04 mg ml^{-1} pronase, Sigma). The cells were finally suspended in Hepes-buffered Dulbecco's modified Eagle's medium and left at room temperature (18–21 °C) until use. Only myocytes displaying a rod shape and calcium tolerance were used in the study.

Measurement of intracellular pH

SNARF loading and calibration. The pH_i of single isolated myocytes was measured using carboxy-SNARF-1, a dual-emission pH-sensitive fluoroprobe (Buckler & Vaughan-Jones, 1990). Cells were loaded by incubation in a 10–20 μM solution of carboxy-SNARF-1-AM ester at room temperature for 5–10 min. Carboxy-SNARF-1 fluorescence from individual cells was excited at 540 ± 12 nm and measured simultaneously at 590 ± 5 and 640 ± 5 nm with an inverted microscope (Nikon Diaphot) converted for epifluorescence. The signals were then digitized at 0·5 kHz (CED 1401). The emission ratio of 590 nm/640 nm was calculated and converted to a pH value using pH calibration data for SNARF, obtained *in situ* (see below) in combination with the following equation:

$$pH = pK_a - \log((R - R_{min})/(R_{max} - R)) - \log F_{640,max/min},$$

where R is the fluorescence emission ratio 590 nm/640 nm; R_{max} is the emission ratio at low pH (5·5), i.e. when the fluoroprobe is predominantly in the protonated form; R_{min} is the emission ratio at high pH (9·5), i.e. when the fluoroprobe is predominantly in the non-protonated form; $F_{640,max/min}$ is the ratio of fluorescence measured at 640 nm for high pH to that for low pH; see Buckler & Vaughan-Jones (1990) for further details. Calibration of SNARF *in situ* was achieved using the nigericin technique (e.g. Lagadic-Gossmann *et al.* 1992*a*). Briefly, a cell loaded with SNARF was exposed, at the end of an experiment, to calibration solutions containing 10 μM nigericin. The solution composition was (mM): 140 KCl, 1 $MgCl_2$, 0·5 EGTA and 20 Hepes for pH 7·5, 20 Mes for pH 5·5, or 20 CAPSO (3-(cyclohexylamino)-2-hydroxy-1-propanesulphonic acid) for pH 9·5. Each pH was adjusted with NaOH.

Stability of a pH_i recording. This was checked before starting an experiment and only those cells whose initial pH_i drifted by $<0·007$ pH units min^{-1} were accepted. In most accepted cases, initial pH_i drift was much less than this. For example, in the experiments illustrated in the present paper (excluding Figs 3*A*, 7*C* and 9, where initial pH_i was still recovering from a previous manoeuvre), initial pH_i drift was 0·0011 ± 0·0006 pH units min^{-1} ($n = 14$). The cause of pH_i drift is not known, but it was not due to light-induced dye bleaching since, when it occurred, it proceeded at the same rate irrespective of whether the cell was illuminated briefly every minute or continuously. Other forms of photodynamic damage are also unlikely because (i) cell illumination intensity was always minimized by placing a 1000-fold neutral-density filter in front of the 100 W xenon excitation lamp and (ii) there was no evidence of light-induced sarcolemmal blebbing in the cells. Although not tested rigorously, it was our impression that pH_i drift occurred less often in cells bathed with CO_2–HCO_3^--buffered solutions, which may suggest a requirement of the cells for HCO_3^- transport for the efficient long-term control of pH_i.

Cleaning the superfusion system. Following calibration, great care was taken to remove nigericin contamination of the superfusion system, a procedure essential for avoiding potential nigericin contamination of cells used in subsequent experiments (Richmond & Vaughan-Jones, 1993). The tubes and superfusion lines (mainly of stainless steel with silicone rubber connectors), the experimental chamber and the solution-switching tap were irrigated continuously for several hours with a 2% solution of bovine albumen (Sigma), then for 12 h with a warm (60 °C) 20% solution of detergent (Decon 75, Decon Laboratories Ltd, Sussex, UK), followed by several hours of flushing with ethanol. Finally, the system was perfused for several hours with distilled water.

Default calibration data. Because the washing procedure was so extensive, nigericin calibrations could not be undertaken after every experiment. Instead, groups of calibrations on more than ten cells were performed about once a month, in order to generate average *in situ* values for R_{max}, R_{min} and the ratio for pH 7·5 plus an average value for $F_{640,max/min}$. From these values, the true pK_a of SNARF was also calculated. The averaged values were then used as default values for the calibration of intracellular fluorescence ratios in subsequent experiments. A typical set of default values used for calibration calculations is: R_{max}, 1·66 ± 0·03; R_{min}, 0·16 ± 0·01; $F_{640,max/min}$, 2·16 ± 0·26; pK_a, 7·52 ± 0·04 ($n = 13$).

The accuracy of the *in situ* nigericin calibration was cross-checked regularly during experiments, using the weak acid–weak base (propionate–trimethylamine) null-point technique (Eisner, Kenning, O'Neill, Pocock, Richards & Valdeolmillos, 1989; see also Buckler & Vaughan-Jones, 1990, for details of the experimental procedure). An acceptable cross-check was one where the null-point technique and the nigericin default calibration data produced estimates of resting pH_i in a myocyte that differed by no more than 0·1 pH units (in practice, agreement was more commonly to within 0·05 pH units). Finally, the pH_i signal used for display of experimental results, was averaged over 0·5 s intervals.

Voltage clamp

Voltage-clamp recordings were performed using the nystatin perforated-patch, whole-cell configuration technique. Electrodes were fabricated from thin-walled borosilicate glass capillaries (GC120-TF, Clarke Electromedical) without polishing. The internal filling solution contained (mM): 140 potassium gluconate, 10 NaCl, 10 Hepes, 1 EGTA and 5 $MgCl_2$. pH values were adjusted to 7·3 at room temperature with KOH. For perforated-patch experiments, 1 mg ml^{-1} nystatin was added directly to this solution. The electrodes had a resistance of 3–5 MΩ when filled with the solution. Membrane potential and current were measured using an Axopatch-1D amplifier, filtered at 1 kHz and digitized at 250 Hz.

Solutions

Hepes- or Pipes-buffered Tyrode solutions (nominally free of CO_2–HCO_3^-) contained (mM): 140 NaCl, 4·5 KCl, 1 $MgCl_2$, 2·5 $CaCl_2$, 11 glucose and 20 Hepes ($pK_a = 7·5$) for pH 7·4 or Pipes (1,4-piperazinediethane sulphonic acid, $pK_a = 6·8$) for pH 6·4; pH was adjusted to 7·4 or 6·4, respectively, at 37 °C with NaOH. For a few experiments (see Fig. 1*B*), solution pH was titrated to 8·40. In

this case, the solution contained 20 mM Hepps (*N*-(2-hydroxyethyl)piperazine-*N*′-(3-propane-sulphonic acid), $pK_a = 8{\cdot}0$). In Na^+-free Tyrode solution, Na^+ was replaced with 140 mM *N*-methyl-D-glucamine (NMDG); pH adjusted to 7·4 or 6·4 at 37 °C with HCl. In high-K^+ Tyrode solution, 115 mM NaCl was replaced with 115 mM KCl. Cl^--free Tyrode solution contained (mM): 140 aspartate, gluconate or glucuronate (Na^+ salt), 4·5 potassium gluconate, 4 calcium gluconate (hemicalcium salt), 1 $MgSO_4$, 11 glucose and 20 Hepes or Pipes; pH adjusted to 7·4 or 6·4, respectively, at 37 °C with NaOH. Na^+-free, Cl^--free Tyrode solution contained (mM): 140 NMDG, 4·5 potassium gluconate, 4 calcium gluconate (hemicalcium salt), 1 $MgSO_4$, 11 glucose and 20 Hepes or Pipes; pH adjusted to 7·4 or 6·4 at 37 °C with glucuronic acid.

HCO_3^--buffered Tyrode solutions were saturated with 5% CO_2–95% O_2. The basic solution contained (mM): 120 NaCl, 4·5 KCl, 1 $MgCl_2$, 2·5 $CaCl_2$, 11 glucose; pH was adjusted to 7·4 or 6·4 at 37 °C with $NaHCO_3$ (usually about 20 and 2 mM, respectively). In some initial experiments using HCO_3^--buffered media, the pH_o 6·4 solutions also contained 20 mM Pipes, but in later work this was omitted; this had no significant influence on the results. For a few experiments (see Fig. 1*B*), solution pH was raised to 8·0 by adding further $NaHCO_3$ (to a final concentration of about 60 mM). In this case, NaCl was simultaneously reduced to 80 mM in order to maintain constant osmolarity. For Na^+-free, HCO_3^--buffered Tyrode solution, Na^+ was replaced with NMDG, and pH adjusted to 7·4 or 6·4 at 37 °C with HCl. For high-K^+, HCO_3^--buffered Tyrode solution, 110 mM NaCl was replaced with equimolar KCl, and pH adjusted to 7·4 or 6·4 at 37 °C with $KHCO_3$. The Cl^--free, HCO_3^--buffered solution contained (mM): 140 aspartate, gluconate or glucuronate (Na^+ salt), 4·5 potassium gluconate, 4 calcium gluconate (hemicalcium salt), 1 $MgSO_4$, 11 glucose, pH was adjusted to 7·4 or 6·4 at 37 °C with $NaHCO_3$. Na^+-free, Cl^--free, HCO_3^--buffered Tyrode solution contained (mM): 140 NMDG, 4·5 potassium gluconate, 4 calcium gluconate (hemicalcium salt), 1 $MgSO_4$, 11 glucose, pH was adjusted to 7·4 or 6·4 at 37 °C with glucuronic acid.

Amiloride, DIDS (4,4′-diisothiocyanatostilbene-2,2′-disulphonic acid), iodoacetate or DBDS (4,4′-dibenzamidostilbene-2,2′-disulphonic acid, disodium salt) were added directly to the solutions. All chemicals were purchased from Sigma except carboxy-SNARF-1-AM and DBDS which were purchased from Molecular Probes. All statistical data are expressed as means ± S.E.M.

Calculation of net sarcolemmal acid flux

Net acid influx (J_H) initiated by reducing pH_o was calculated from the fall of pH_i, using the equation:

$$J_H = \beta_{tot} \times dpH_i/dt.$$

The value for dpH_i/dt was obtained by a linear fit of the initial pH_i fall 0·5–2·0 min (or 0·5–3·0 min) following the reduction of pH_o. The pH_i fall between these time markers was invariably linear and was best fitted by computer as a least-squares regression line to the calibrated pH_i trace, with data points sampled at 0·5 s intervals. The pH_i at which dpH_i/dt was measured was taken (by computer) as the midpoint pH_i for the range used in the best-fit procedure. β_{tot} is total hydrogen ion buffering capacity in the cells and was obtained from the summation of β_i (intrinsic buffering power) and β_{CO_2} (buffering power caused by intracellular CO_2–HCO_3^-). β_i and β_{CO_2} were obtained from the following equations:

$$\beta_i = -28 \times pH_i + 222{\cdot}6,$$

(this is the empirical equation determined by Lagadic-Gossmann *et al.* 1992*a*, as a least-squares linear regression fit to their experimentally determined dependence of β_i on pH_i in the ventricular myocyte);

$$\beta_{CO_2} = 2{\cdot}3 \times [HCO_3^-]_i = 2{\cdot}3 \times [HCO_3^-]_o \times 10^{(pH_i - pH_o)}$$

(this assumes the cell behaves as an open system for CO_2, that the solubility of CO_2 and its apparent pK_a for hydration to form H^+ and HCO_3^- is the same intracellularly as it is in extracellular solution, and that CO_2 hydration and transmembrane CO_2 distribution is at equilibrium).

When comparing acid-loading fluxes under different experimental conditions, care was taken to ensure that comparison was made at a constant pH_o and also, as near as possible, at a common pH_i. In all the comparisons shown in the present work, pH_i differed in control *versus* test, by no more than 0·05, except for the case shown in Fig. 12*B*, where the control flux (labelled Normal $[Cl^-]_o$) was measured at an average pH_i which was 0·078 ± 0·012 pH units ($n = 13$) more acid than in the test (labelled Zero $[Cl^-]_o$). This pH_i difference is still small and would not affect the conclusion drawn from the data.

RESULTS

Effect on pH_i of changing pH_o

Figure 1 illustrates the effect on pH_i of reducing pH_o. In Fig. 1*A*, the experiment was performed in the nominal absence of CO_2, by using a superfusate buffered with 20 mM Hepes or 20 mM Pipes to a pH_o of 7·4 and 6·4, respectively. The first part of the experiments shown in Figs 9 and 11 also illustrates a similar manoeuvre, but under conditions where the superfusate was buffered with 5% CO_2 and 20 mM HCO_3^- (pH_o 7·4) or 2 mM HCO_3^- (pH_o 6·4) instead of Hepes/Pipes. In all cases, reducing pH_o initiated a reversible fall of pH_i. In other experiments (not illustrated) raising pH_o (to 8·0 or 8·40) produced a reversible rise of pH_i. The value of pH_i 10–15 min after changing pH_o is plotted in Fig. 1*B*. The pH_o dependence of pH_i is essentially linear over the pH_o range tested.

The relationship in HCO_3^--buffered medium, plotted in Fig. 1*B*, is displaced downwards (by about 0·2 pH units) relative to that plotted for HCO_3^--free conditions. This indicates a lower resting pH_i in CO_2–HCO_3^- compared with Hepes. In other experiments, such a pH_i discrepancy was not always observed; for example, removal of CO_2–HCO_3^- in the experiment shown in Fig. 9*A* resulted in a rise of pH_i, but after a few minutes pH_i was recovering to a value similar to that seen before CO_2–HCO_3^- removal. A discrepancy between pH_i of ventricular tissue bathed in HCO_3^--containing and HCO_3^--free media has been variably reported in the past; compare Vanheel & de Hemptinne (1985), Bountra, Powell and Vaughan-Jones (1990), and Lagadic-Gossmann *et al.* (1992*a*), where little or no discrepancy was observed, with Blank *et al.* (1992) where a discrepancy of 0·34 pH units was found. The reason for this variability is not known, but a lower pH_i in CO_2–HCO_3^- buffer has been suggested to be caused by activation in this buffer system of a HCO_3^- efflux mechanism (Vaughan-Jones, 1979*b*; Vanheel & de Hemptinne, 1985; Blank *et al.* 1992).

The important point to note in Fig. 1*B* is that the *sensitivity* of pH_i to pH_o (i.e. slope of relationship) is not affected greatly by the presence or absence of CO_2–HCO_3^-, despite the fact that addition of 5% CO_2–HCO_3^- greatly increases

the intracellular H^+-buffering power of the cell. The sensitivity of pH_i to pH_o is such that a 1·0 unit fall of pH_o lowers pH_i by about 0·4 pH units. The remainder of this paper addresses the mechanism underlying the fall of pH_i with pH_o. For convenience, the experimental work is divided into two sections. Part I presents experiments carried out in the nominal absence of CO_2–HCO_3^- buffers (to eliminate bicarbonate-dependent pH effects), Part II presents similar experiments performed in the presence of a 5% CO_2–HCO_3^--buffer system.

Part I: acid loading in bicarbonate-free media

Effect of inhibiting Na^+–H^+ exchange

Amiloride addition. One possible mechanism for the fall of pH_i in low pH_o is that Na^+–H^+ exchange (NHE) is inhibited by extracellular acidosis (e.g. Vaughan-Jones & Wu, 1990), revealing a background acid-loading mechanism which then reduces pH_i. Figure 2 shows experiments which indicate that this cannot be the main mechanism. Because the experiments were performed in HCO_3^--free solutions, NHE will have been the only functional acid extruder (Lagadic-Gossmann *et al.* 1992*a*). Figure 2*A* shows that addition of 1·5 mM amiloride, an inhibitor of cardiac NHE, acidified the cell, but the rate of fall of pH_i was considerably less than that observed upon lowering pH_o to 6·40 (in the absence of amiloride). On average, the initial rate of acidosis in pH_o 6·40 was 0·060 ± 0·002 pH units min^{-1} ($n = 49$), more than threefold faster than that seen in amiloride applied at pH_o 7·40 (0·015 ± 0·001 pH units min^{-1}, $n = 33$). Evidence that amiloride was indeed fully inhibiting NHE came from the observation that, after a period in low pH_o, restoring pH_o to 7·40 caused a recovery of intracellular pH, and this recovery was completely and reversibly inhibited by amiloride (Fig. 2*A*; similar result in 3 other experiments). These data therefore indicate that attenuation of NHE activity by low pH_o, although it must occur, cannot account for the majority of the acid-induced fall of pH_i.

It is notable in Fig. 2*A* that the fall of pH_i in amiloride (pH_o 7·40) was *accelerated* by reducing pH_o to 6·40. This is seen more clearly in Fig. 2*B* (1 of 3 similar experiments) which shows that amiloride application at pH_o 7·40 exerted little effect on resting pH_i (indicating that, in this cell, resting background acid loading was low). Following reduction of pH_o, the intracellular pH decreased and stabilized at 6·78. Addition of amiloride under these conditions then revealed a rapid fall of pH_i, and hence a large background acid loading. In other words, acid loading (normally balanced in the steady state by acid extrusion on Na^+–H^+ exchange) must have been stimulated by the reduction of pH_o.

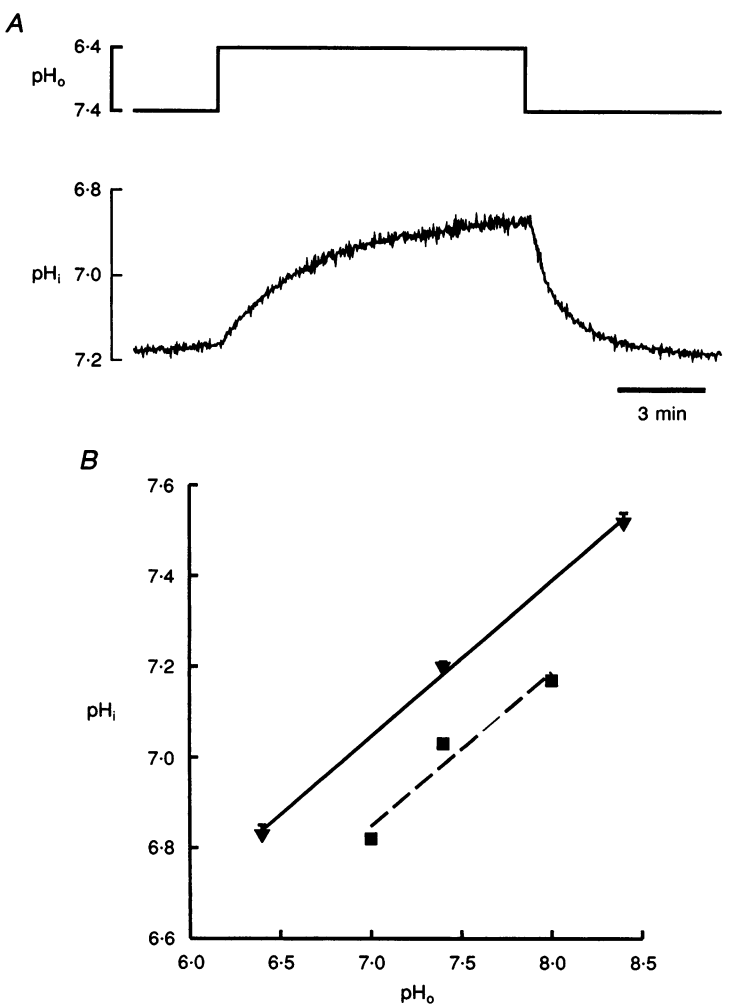

Figure 1. The pH_o dependence of pH_i
A, pH_i fall in low pH_o in a single ventricular myocyte bathed in nominally CO_2–HCO_3^--free Tyrode solution. Extracellular pH was changed from 7·4 (20 mM Hepes buffer) to 6·4 (20 mM Pipes buffer) as indicated by the bar above the pH_i trace. *B*, ▼, data (± S.E.M.) obtained in CO_2–HCO_3^--free conditions at pH_o 6·4 ($n = 34$), 7·4 ($n = 164$) and 8·4 (Hepps buffer, $n = 14$). ■, data from 5% CO_2–HCO_3^--containing solution buffered to 7·0, 7·4 and 8·0 ($n = 4$ for each point; pH_o achieved by varying $[HCO_3^-]_o$, see Methods). Continuous and dashed lines fitted by linear least-squares regression analysis. All measurements of pH_i following extracellular acidosis or alkalosis were made 10–15 min after the change of pH_o.

Na^+ removal. In the first part of the experiment shown in Fig. 2*C*, a cardiomyocyte had been exposed for 40 min to a Na^+-free solution (NMDG substituted). Under these conditions Na_i^+ is also likely to have fallen to low levels (Ellis, 1977). Reduction of pH_o to 6·40 still produced a fall of pH_i. Indeed the initial fall was about 20% faster than that seen under normal Na^+-containing conditions ($P < 0·05$, $n = 5$; Student's paired t test). This provides final proof that acid loading is not merely due to modulation of NHE activity since such activity would already be zero in Na^+-free conditions.

Effect of the stilbenes, DIDS and DBDS

In order to remove the possibility of sarcolemmal HCO_3^- carriers affecting pH_i by operating with residual levels of cellular HCO_3^- (Vanheel, de Hemptinne & Leusen, 1984; Vaughan-Jones, 1986), we added the stilbene drug DIDS which inhibits HCO_3^- transport in heart (Vaughan-Jones, 1986; Lagadic-Gossmann *et al.* 1992*a*). Figure 3*A* shows that the low-pH_o-induced fall of pH_i was unaffected by 0·5 mM DIDS ($n = 9$). In other experiments, a cell was exposed to DIDS (0·1–0·5 mM) for 2–10 min (mean exposure, 5·9 ± 1·6 min; $n = 7$) to determine possible effects on resting pH_i. No significant effect was seen, pH_i fell in DIDS by 0·0014 ± 0·008 ($P > 0·05$). Subsequent reduction of pH_o to 6·40 again produced a fall of pH_i similar to that seen in the absence of DIDS. We conclude that, in Hepes-buffered media, the pH_i fall is independent of the known HCO_3^- transporters.

In contrast to the lack of effect of DIDS, the rate of fall of pH_i in low pH_o was slowed greatly in the presence of another stilbene compound, DBDS, as shown in Fig. 3*B*. DBDS inhibits a variety of anion tranporters, including the lactic acid carrier (Poole & Halestrap, 1993). A 0·2 mM dose, which is close to the maximum solubility of the drug,

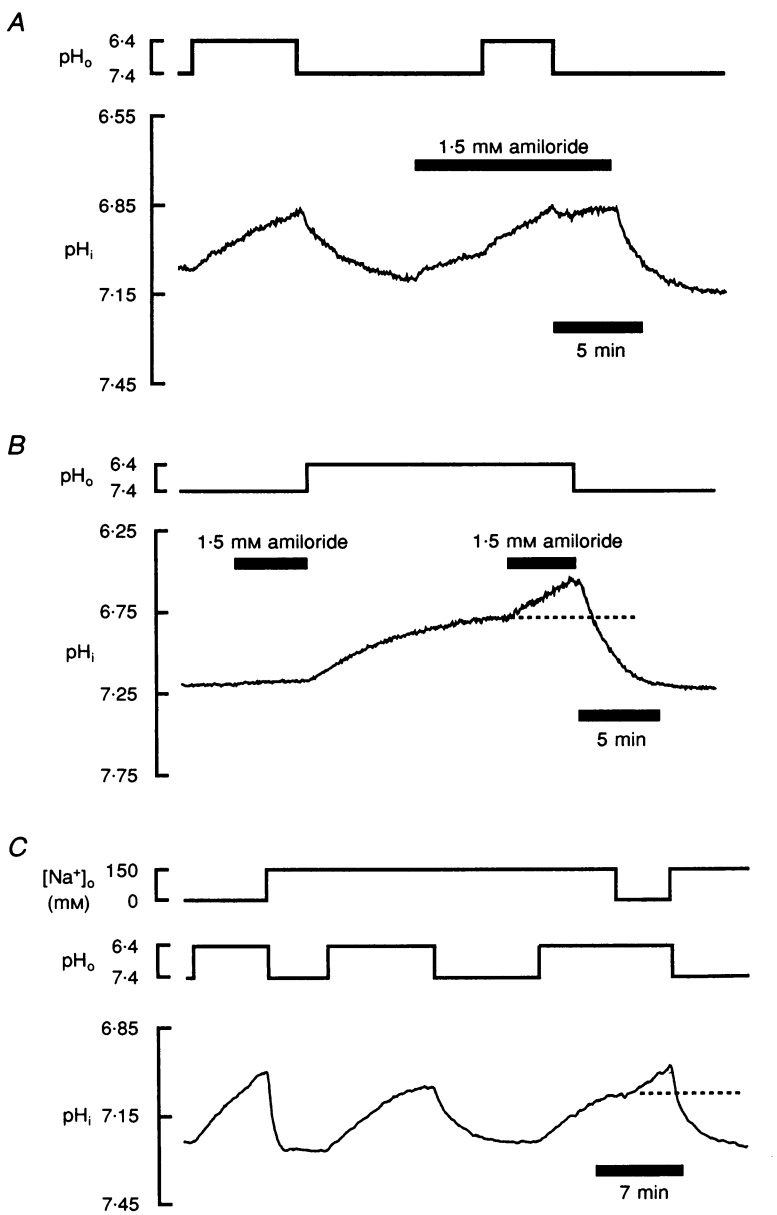

Figure 2. Effect of amiloride and Na_o^+ removal on acid loading in low pH_o (HCO_3^--free conditions)

A, amiloride: changes of pH_o indicated at top of trace; amiloride application indicated by filled bar. *B*, in this experiment, amiloride was added before and after the reduction of pH_o (the latter addition made after pH_i had fallen). Dotted horizontal line drawn to facilitate viewing of amiloride-induced fall of pH_i in low-pH_o solution. *C*, Na_o^+ removal: Na_o^+ replaced by NMDG, as indicated at top of panel; trace below this indicates changes of pH_o. Note that, towards the end of the experiment, removal of Na_o^+ (after stabilization of pH_i in 6·4 pH_o) restored the fall of pH_i to a rate similar to that seen in pH_o 6·4, Na^+-free solution at the beginning of the experiment.

inhibited the fall of pH_i (measured over a 6–10 min period in low pH_o) by 70·4 ± 4·1 % ($n = 6$).

Effect of inhibition of lactate transport

Because of the inhibitory effect of DBDS, we tested if modulation of lactic acid transport was involved in the fall of pH_i. Figure 4*A* shows that α-cyano-4-hydroxycinnamate (CHC, 5 mM), an inhibitor of lactate–H^+ symport in cardiac cells (Poole & Halestrap, 1993), failed to inhibit the fall of pH_i in low pH_o. A similar result was seen in five other cells. Note that CHC itself induced an intracellular acidosis of about 0·1 pH units ($n = 6$).

We also tested (Fig. 4*B*) for possible involvement of lactate transport by applying the glycolytic inhibitor, iodoacetate (IAA; 0·5 mM) in a glucose-free solution, in order to inhibit lactic acid generation. This would remove the substrate for any sarcolemmal lactate transport. In six cells, pretreatment with this agent for up to 10 min failed to inhibit the fall of pH_i in low pH_o (e.g. Fig. 4*B*). A similar result was obtained when we used 10 mM deoxyglucose (DOG up to 10 min application in a glucose-free solution) instead of IAA to reduce the intracellular production of lactate ($n = 6$; data not shown).

Results with CHC, IAA and DOG indicate that modulation of lactate transport by pH_o is unlikely to account for the acid-induced fall of pH_i.

Effect of changing membrane potential or extracellular K^+

Two possible sources of acid loading that may operate in nominally HCO_3^--free conditions are (i) K^+-dependent acid influx through a K^+–H^+ exchanger (e.g. Maldonado & Cala, 1994), acid loading being driven by the outward K^+ gradient, and (ii) acid equivalent influx through H^+ conductance channels (Thomas & Meech, 1982) although these usually display strong outward rectification. Figure 5, one of eight similar experiments, shows that elevating K_o^+ from 4·5 to 115 mM (thus reducing the outward K^+ gradient) had no effect on the rate of fall of pH_i in low pH_o, indicating that acid loading is not a K^+-dependent process.

The lack of effect of changing K_o^+ would also suggest that the acid loader is not a voltage-driven process. We confirmed this by subjecting a myocyte to whole-cell voltage clamp, using a nsytatin-based perforated-patch technique, while simultaneously recording pH_i. Figure 6 shows one of eight similar experiments. Depolarizing the holding

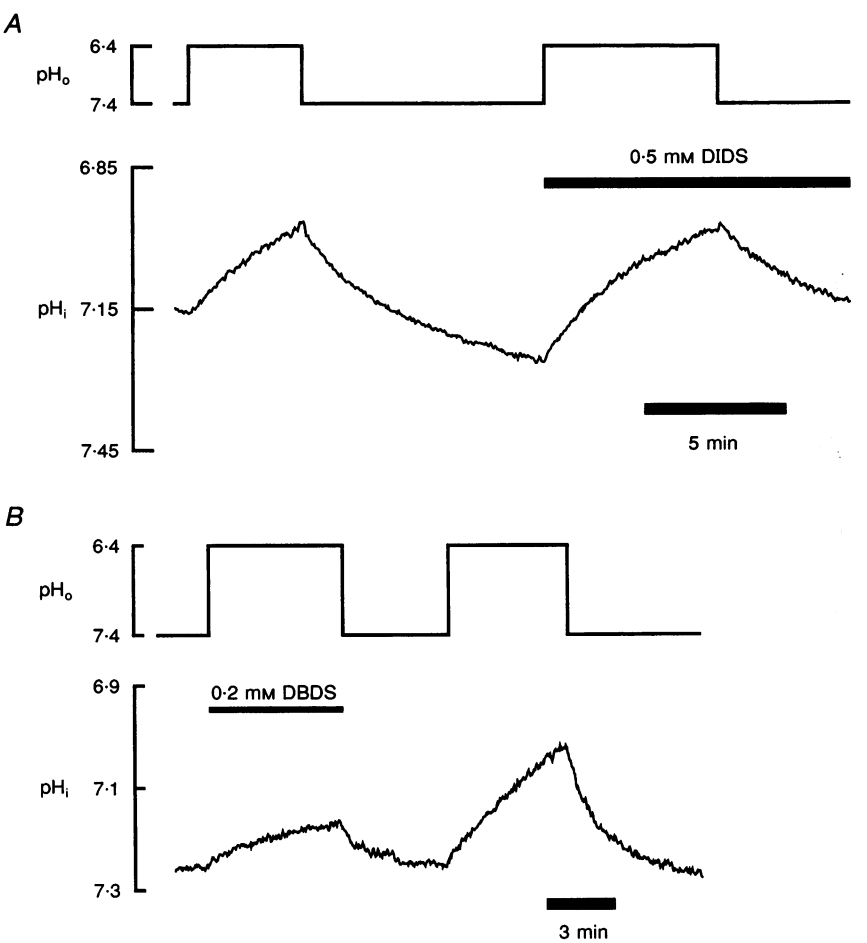

Figure 3. Effect of stilbenes on acid loading in low pH_o (HCO_3^--free conditions)

A, effect of DIDS. Trace begins towards the end of a previous recovery from a period in low pH_o. *B*, effect of DBDS.

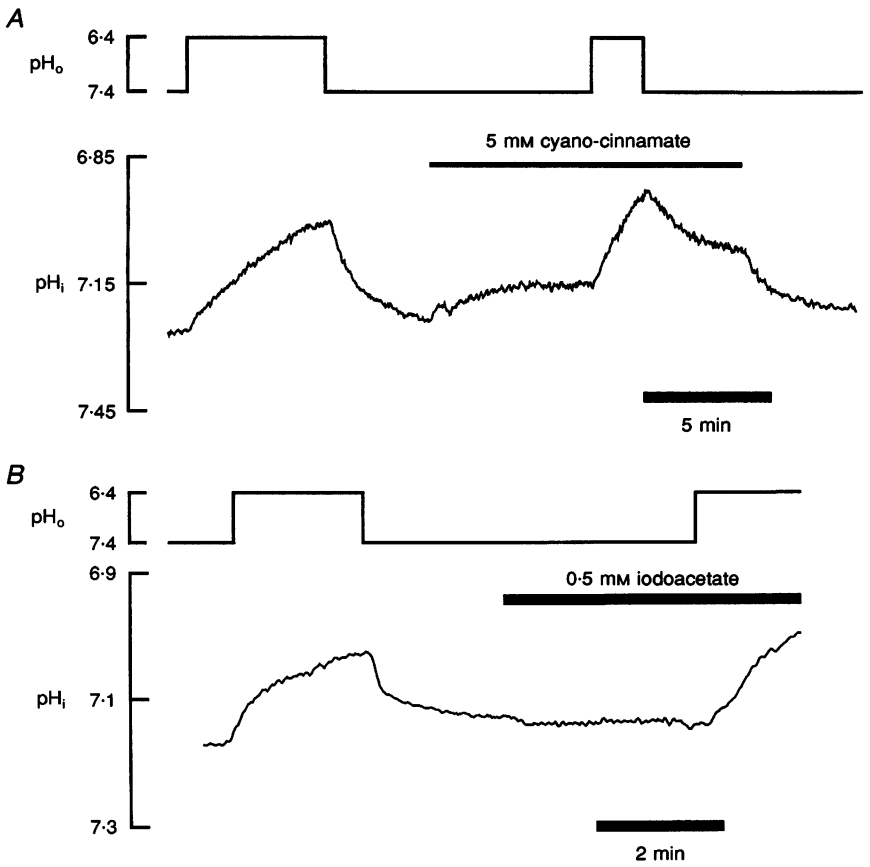

Figure 4. Effect of inhibiting lactate transport and glycolysis (HCO_3^--free conditions)
A, effect of cyano-cinnamate (lactate transport inhibitor). *B*, effect of 0·5 mM iodoacetate (glycolytic inhibitor).

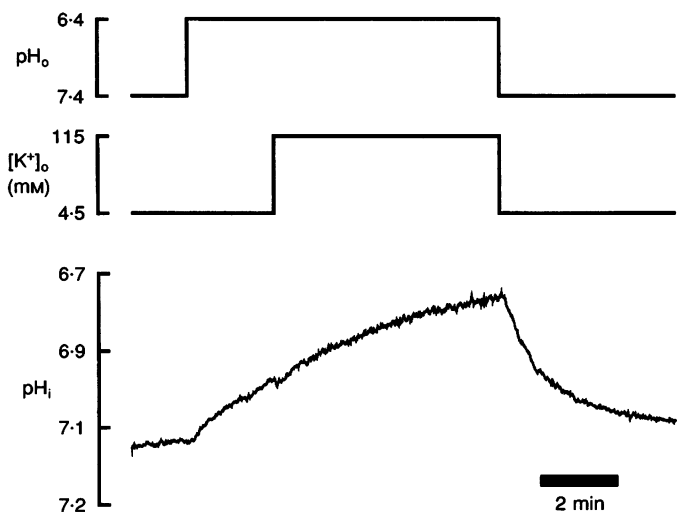

Figure 5. Effect of high K_o^+ (HCO_3^--free conditions)
K_o^+ was elevated by isosmotic substitution for NMDG in a low-Na^+ solution (see Methods for full details of solution composition). Change of pH_o indicated at top of figure.

potential from −70 to +70 mV had no effect on the rate of the acid-induced fall of pH_i. A similar result was obtained in all eight experiments. Also shown in Fig. 6, superimposed on the recording of holding potential, is the H^+ equilibrium potential computed from the Nernst equation, using the measured values of pH_i and the value of pH_o. Note that depolarization of the holding potential alters the electrochemical driving force acting on H^+ ions, reversing it from a net inward (at −70 mV) to a net outward direction (at +70 mV). The fact that net acid loading continued in the face of reversal of the electrochemical H^+ gradient indicates that the mechanism of acid loading cannot be via passive H^+ movement through proton channels.

In further experiments (not shown) we found that putative inhibitors of the voltage-gated H^+ channel (Zn^{2+}, Cd^{2+}), the Ca^{2+} channel (Cd^{2+}, Ni^{2+} and diltiazem) and certain K^+ channels (Ba^{2+}, 1 mM) (1 mM Zn^{2+}, $n = 5$; 5 mM Cd^{2+}, $n = 6$; 1 mM diltiazem, $n = 5$; 5 mM Ni^{2+}, $n = 5$; 1 mM Ba^{2+}, $n = 5$, respectively), also failed to affect the rate or magnitude of low-pH_o-induced acid loading in the cardiomyocyte.

Effect of Cl_o^- removal

The acid-induced fall of pH_i requires extracellular Cl^-. This is shown in Fig. 7 where short-term substitution of extracellular Cl^- (<5 min before reducing pH_o) by glucuronate (Fig. 7*A*) or gluconate (Fig. 7*B*) inhibited reversibly the acid-induced fall of pH_i. The inhibitory effect of a Cl^--free solution was independent of the time of exposure to the solution. This is indicated by comparison of Fig. 7*A* and *B* (short-term Cl_o^- removal) with the results illustrated in Fig. 7*C*, where a cell had been exposed to zero Cl_o^- (glucuronate substituted) for over 30 min before testing the effect of reducing pH_o. As with short-term Cl_o^- removal, the acid-induced fall of pH_i was largely inhibited, and the effect was rapidly reversed following readmission of Cl_o^-. A similar result was seen in six other cells. Since Cl_i^- in cardiac tissue is reduced to low levels after 30–40 min in Cl^--free solution, whereas it is little affected by short-term Cl_o^- removal (Vaughan-Jones, 1979; Desilets & Baumgarten, 1986), the results shown in Fig. 7*A–C* indicate that Cl_o^- but not Cl_i^- is a necessary requirement for the acid-induced fall of pH_i.

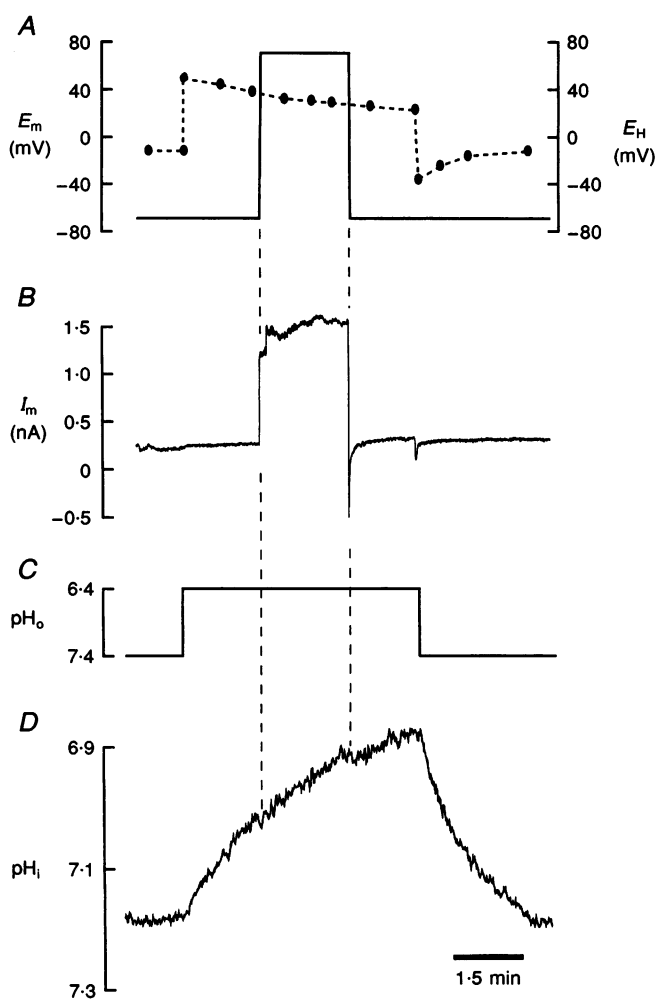

Figure 6. Effect of reversing electrochemical H^+ gradient (HCO_3^--free conditions)

Traces show voltage-clamped membrane potential (*A*; whole-cell perforated patch: nystatin), membrane current (*B*), extracellular pH (*C*) and intracellular pH (*D*). Value of E_H (proton equilibrium potential) computed from pH_o and pH_i (using the Nernst equation) is plotted (in millivolts) relative to the membrane potential in *A* (●, dashed line). See text for details.

Figure 8 summarizes the effects on the pH_i fall in low pH_o, of using various Cl^- substitutes. Replacement of Cl_o^- with gluconate or glucuronate, removed 85% of acid loading. Inhibition was a little less when using aspartate; here the pH_i fall was inhibited by 80% (Fig. 8*A*). A similar picture emerged upon examination of the inhibitory effect of Cl^- substitutes on the initial rate of fall of pH_i upon pH_o reduction (Fig. 8*B*), again with inhibition in aspartate being slightly less than that seen in the other two Cl^- substitutes. Possible reasons for the reduced inhibition in aspartate are considered in the Discussion. Overall, the results shown in Fig. 8 indicate that acid loading in HCO_3^--free conditions is largely a Cl^--dependent process.

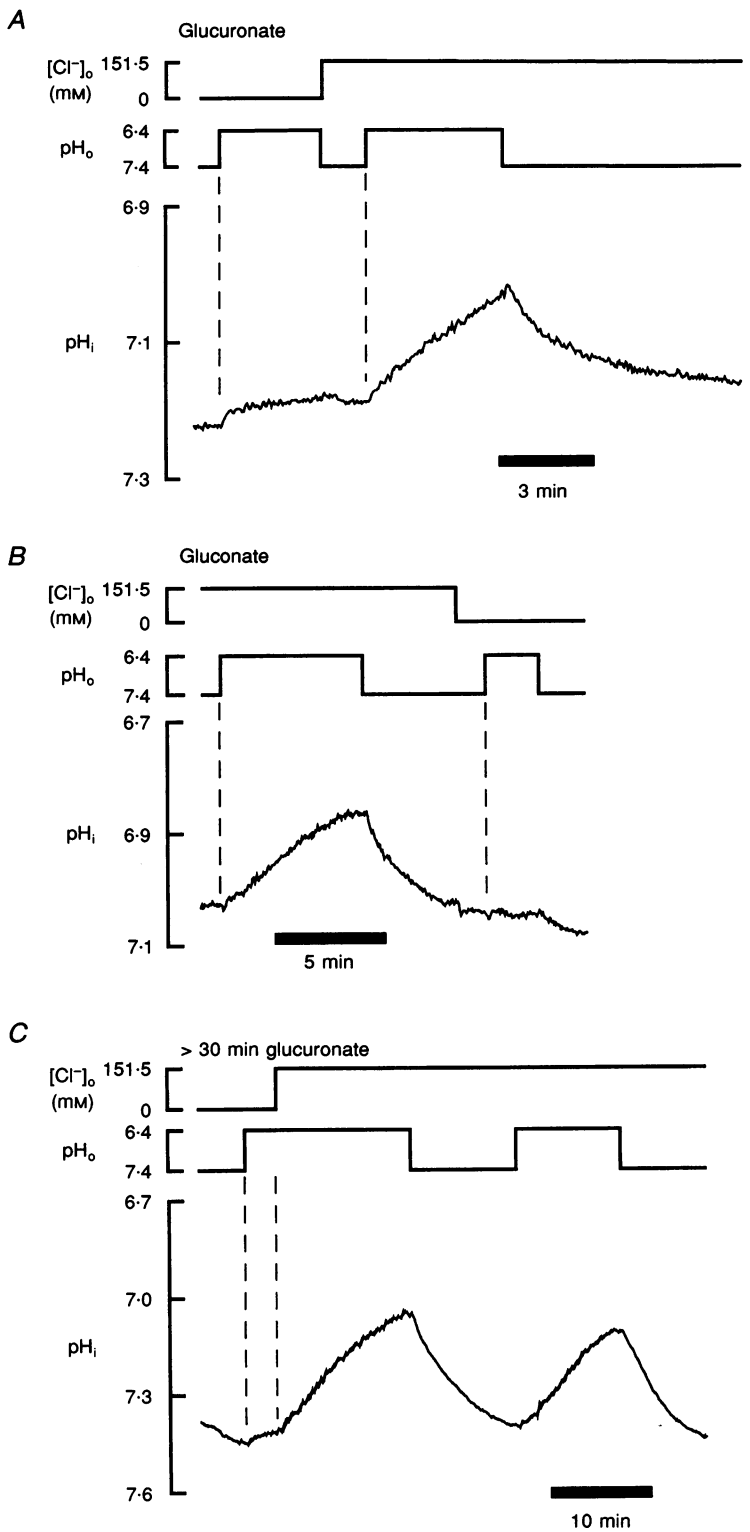

Figure 7. Removal of Cl_o^- inhibits acid loading

A and *B* show effect of short-term Cl_o^- removal (<5 min before pH_o reduction) on low-pH_o-induced acid loading; Cl_o^- replaced isosmotically by glucuronate (*A*) or gluconate (*B*). Each panel also shows a control fall of pH_i induced by low pH_o in the presence of full Cl_o^-. *C* shows that longer pretreatment in Cl^--free solution (>30 min; glucuronate substituted) produced a similar result. At beginning of trace, pH_i was still rising, following the removal of Cl_o^-. Re-adding Cl_o^- in the presence of low pH_o greatly accelerated acid loading.

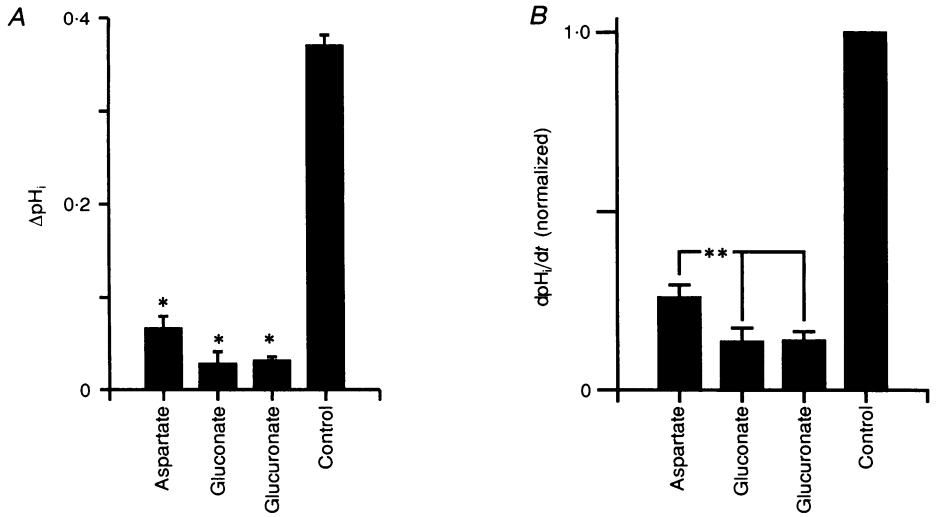

Figure 8. Effect of Cl^- substitutes on acid loading

A, histogram illustrating the pH_i change measured 7–10 min after reducing pH_o to 6·4 in solutions where Cl_o^- was replaced isosmotically by aspartate ($n = 4$), gluconate ($n = 8$) or glucuronate ($n = 12$). * $P < 0{\cdot}001$, Student's paired t test. *B*, histogram of initial rate of fall of pH_i (see Methods) in low-pH_o, Cl^--free solution normalized to that seen (in the same cell) in the presence of full Cl_o^- ; Cl^- substitutes, aspartate ($n = 7$); gluconate ($n = 9$); glucuronate ($n = 14$). ** $P < 0{\cdot}05$ compared with aspartate, Student's unpaired t test.

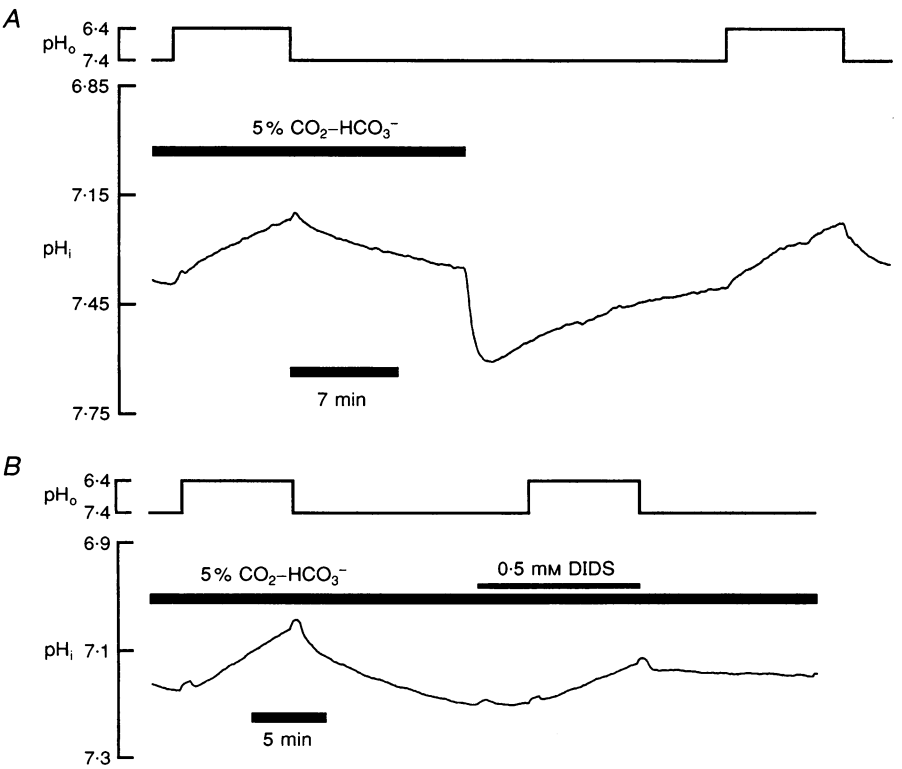

Figure 9. Acid loading is stimulated in the presence of HCO_3^-

A, comparison of acid loading in low pH_o (6·4), 5% CO_2–HCO_3^--containing solution ([HCO_3^-] reduced from 23 to 2·3 mM), with that seen in low-pH_o, nominally HCO_3^--free solution (20 mM Hepes/Pipes buffered). *B*, effect of DIDS on acid loading in HCO_3^--containing solution. Note slowing of loading in DIDS. Note also that pH_i recovery from acidosis was incomplete after DIDS treatment; this was probably caused by DIDS being only partly reversible, coupled with the fact that the drug inhibits not only Cl^-–HCO_3^- exchange, but also the Na^+–HCO_3^- symport in myocytes, a carrier which assists acid extrusion. At the start of traces shown in both *A* and *B*, pH_i was approaching a resting level following a previous period in low pH_o (not shown).

Part II: acid loading in CO_2–HCO_3^--buffered media

Dual acid-loading mechanism in the sarcolemma

Hepes *versus* bicarbonate. In the first part of the experiment shown in Fig. 9*A*, pH_o was reduced to 6·4 in HCO_3^--buffered solutions (at constant 5% P_{CO_2}). In the second part, pH_o was again reduced to 6·40, but all solutions were nominally CO_2–HCO_3^- free. Note the transient intracellular alkalosis upon switching from CO_2–HCO_3^- to Hepes-buffered solution. This is caused by exit of CO_2 from the cell, while the subsequent pH_i recovery from the alkali load is caused by sarcolemmal acid-loading mechanisms (see Discussion).

The first couplet of the histogram shown in Fig. 10*A* quantifies initial net acid influx in low pH_o and shows that acid loading in CO_2–HCO_3^- conditions is about twice as large as that in Hepes. Thus acid loading is *stimulated* in the presence of HCO_3^-.

Effect of DIDS. The experiment illustrated in Fig. 9*B* shows that, in the presence of CO_2–HCO_3^-, the acid-induced fall of pH_i is slowed by DIDS (0·5 mM), in contrast to the lack of DIDS sensitivity of acid loading observed in Hepes media (Fig. 3). Data from several experiments are summarized in the second couplet of the histogram shown in Fig. 10*A*. DIDS reduced acid influx by about 40%.

Figure 10*B* compares the magnitude of acid loading in low-pH_o Hepes with the DIDS-insensitive fraction of acid loading estimated under CO_2–HCO_3^- conditions. The two fractions are not statistically different ($P > 0·05$). This suggests strongly that, in the presence of a CO_2–HCO_3^--buffer system, the novel acid loader described in Part I remains functional and contributes 50–60% of acid-equivalent influx during low pH_o exposure. The other 40–50% of acid loading is contributed by a HCO_3^--activated mechanism which is DIDS inhibitable. The identity of this latter process is investigated below.

Ionic dependence of acid loading in CO_2–HCO_3^-

Effect of Na^+ removal. An obvious candidate for the HCO_3^--activated mechanism is the cardiac Cl^-–HCO_3^- exchanger (Vaughan-Jones, 1982). The experiment shown in Fig. 11*A* indicates that the acid-induced fall of pH_i seen under CO_2–HCO_3^- conditions is not inhibited by removal of Na_o^+ (NMDG substituted). As in Hepes-buffered conditions, the rate of fall of pH_i in Na^+-free, HCO_3^--buffered conditions was actually a little faster (by 13%) than that in Na^+-containing conditions ($P = 0·01$; $n = 8$). In contrast, the pH_i recovery from the acid load, initiated by restoring pH_o to 7·40 was, as expected, greatly attenuated in the absence of Na_o^+ (see Fig. 11*A*; similar result seen in 7 other cells). Therefore, as with Hepes/Pipes-buffered solutions (Fig. 3), the acid-loading mechanisms operating in the presence of CO_2–HCO_3^- are *independent* of Na^+.

Effect of raising extracellular K^+. Recent work has demonstrated that, in HCO_3^--buffered conditions, a novel K^+–HCO_3^- co-efflux carrier contributes to acid equivalent loading in the squid giant axon (Zhao, Hogan, Bevensee & Boron, 1995), the energy for HCO_3^- efflux being derived from the outwardly directed K^+ concentration gradient. Figure 11*B*, one of four similar experiments, shows that, when using HCO_3^--buffered solutions, elevation of K_o^+ from 4·5 to 140 mM (and thus abolishing the outward K^+ gradient) had no significant effect on acid loading in low pH_o ($P > 0·05$; $n = 4$). The present results therefore indicate no significant role for K^+–HCO_3^- co-transport.

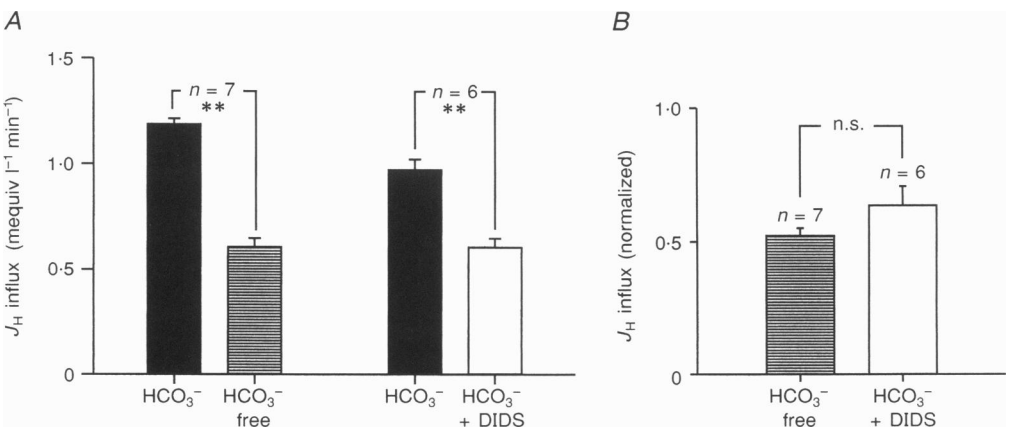

Figure 10. Bicarbonate-stimulated acid loading is DIDS inhibited

A, left couplet: initial rate of acid loading in low pH_o (6·40) in HCO_3^- (■) and in HCO_3^--free conditions (▤). Loading is roughly doubled in HCO_3^--containing conditions. Right couplet: initial loading rate in HCO_3^--containing conditions in the presence (□) and absence (■) of 0·5 mM DIDS. ** $P < 0·001$, paired t test. *B*, HCO_3^--independent acid loading (▤) compared with DIDS-resistant acid loading (□); data taken from *A*, but normalized to the paired rate observed in control HCO_3^--containing conditions (■ in *A*). n.s., not significant ($P > 0·05$).

Effect of Cl^- removal. The experiment illustrated in Fig. 12*A* shows that acid loading in the presence of CO_2–HCO_3^- is greatly attenuated by Cl_o^- removal (gluconate substituted). Towards the middle of the trace, Cl_o^- removal resulted in an intracellular alkalosis, usually attributed to Cl^- efflux in exchange for HCO_3^- ion entry (Vaughan-Jones, 1979; Lagadic-Gossmann *et al.* 1992*a*). The rise of pH_i was beginning to stabilize after about 8 min, whereupon pH_o was reduced to 6·40. This produced a slow acidification of pH_i which rapidly accelerated upon re-admission of Cl_o^- (at pH_o 6·40). A control acid-induced fall of pH_i is shown at the beginning of the trace.

Figure 12*B* pools data from several similar experiments, and shows net acid influx in pH_o 6·40 computed for Cl^--free and Cl^--containing conditions. On average, Cl_o^- removal inhibited acid influx by 78%. This is a similar fractional inhibition to that seen previously in Cl^--free Hepes conditions (85%; Fig. 8). Since total net acid influx in response to low pH_o, is doubled in HCO_3^- compared with

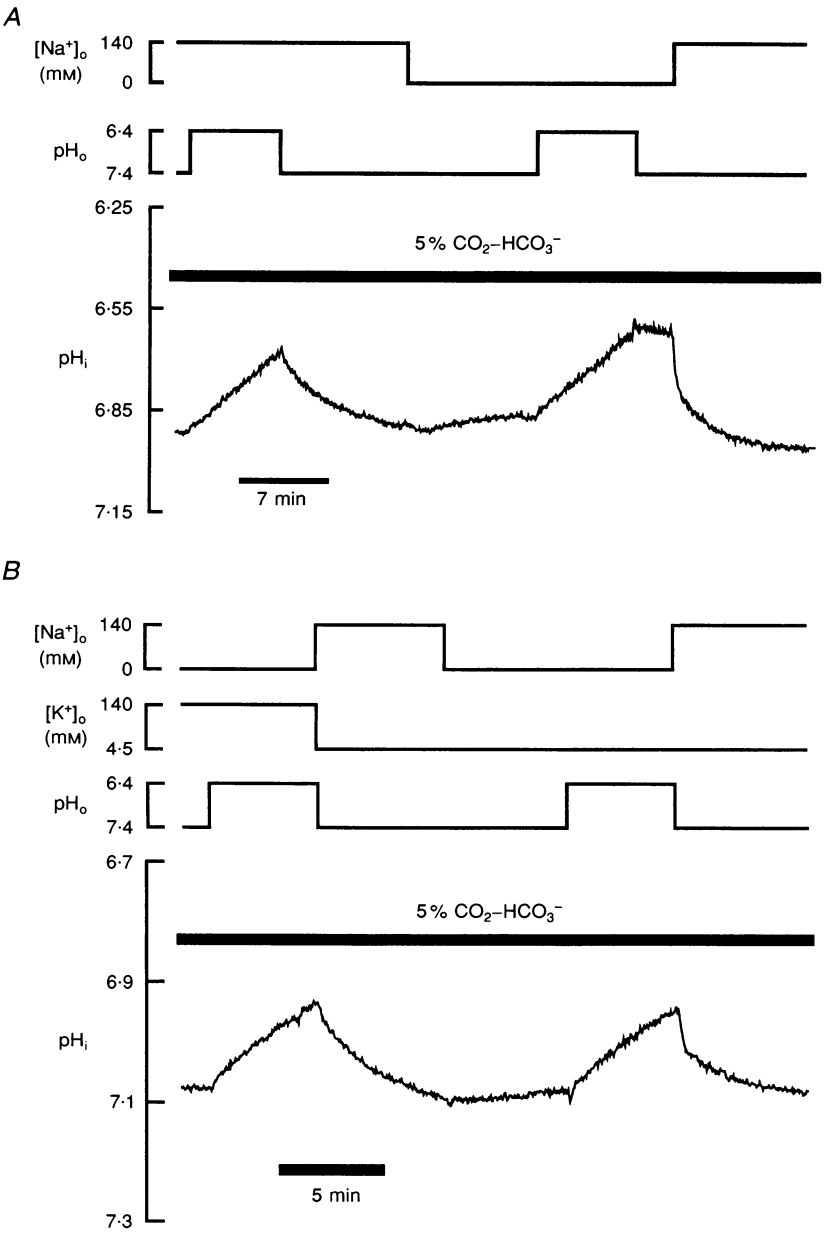

Figure 11. Acid loading in the presence of HCO_3^- is not dependent on Na^+ or K^+

A, effect of Na^+-free solution (NMDG substituted). *B*, effect of high K_o^+ (all Na_o^+ replaced isosmotically by K^+) shown in first part of experiment; second part shows acid loading in the presence of 4·5 mM K^+, Na^+-free solution (Na^+ replaced by NMDG); periods of ionic substitution are indicated by the traces at the top of the figure.

Hepes-buffered conditions, the result shown in Fig. 12*B* indicates that a major fraction of the HCO_3^--activated acid-loading mechanism requires the presence of Cl^-. When combined with the finding that the HCO_3^--activated acid loader is DIDS inhibitable but independent of Na^+, this result provides strong evidence that this acid loader is indeed Cl^-–HCO_3^- exchange.

DISCUSSION

A dual acid-loading mechanism in the mammalian cardiac cell

The present work provides the first evidence for a dual acid-loading mechanism in cardiomyocytes. This system consists of two types of acid-equivalent carrier, both of which are independent of Na^+ and K^+, and both of which are stimulated by reduction of pH_o to produce a fall of pH_i. One of the carriers is Cl^-–HCO_3^- exchange, a carrier known to be involved in acid loading of cardiac cells under other circumstances, specifically following a rise of intracellular pH (Vaughan-Jones, 1982; Xu & Spitzer, 1994). The other element is entirely novel. It is Cl^- dependent and it functions at about the same rate in either the presence or nominal absence of HCO_3^-. In CO_2–HCO_3^--buffered conditions the two carriers contribute roughly equally to the fall of pH_i in low pH_o.

The simplest explanation for the novel acid loader is an H^+–Cl^- co-influx carrier or, alternatively, a Cl^-–OH^- exchanger (CHE). We cannot distinguish between these possibilities but, for convenience, we adopt the latter term (CHE). This is because of (i) the functional similarity of this carrier with the other Cl^--dependent element in the dual acid-loading system, Cl^-–HCO_3^- exchange, (ii) the stilbene sensitivity of CHE (see below), and (iii) the recent identification (see below) of multiple isoforms of anion exchange in mammalian heart.

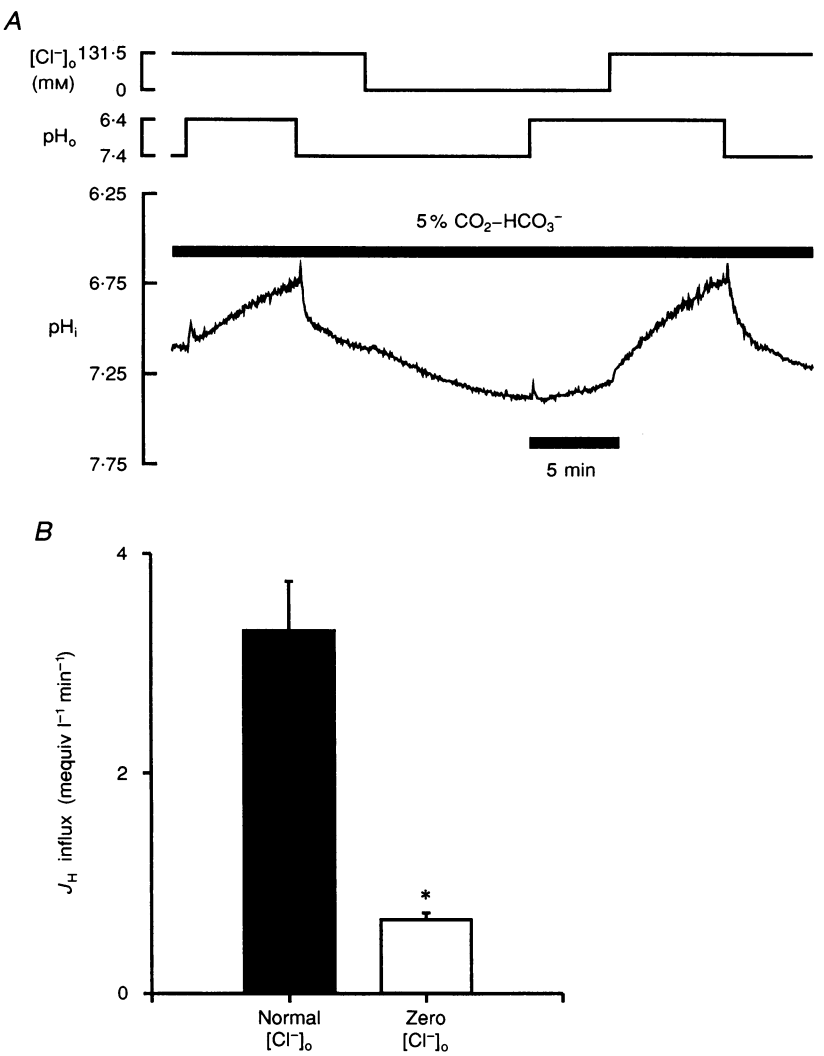

Figure 12. Acid loading in the presence of HCO_3^- is Cl^- dependent

A, experimental protocol; period of removal of Cl_o^- (glucuronate/gluconate substituted) shown at top of figure. *B*, data from experiments like that shown in *A*. Initial acid loading rate in Cl^--free solution (□) and Cl^--containing solution (■); * $P < 0{\cdot}001$, paired t test, $n = 13$.

Cl^-–OH^- exchange is not caused by residual bicarbonate transport. An important question is whether the putative CHE carrier might really be the Cl^-–HCO_3^- exchanger operating, not with OH^- ions, but with residual levels of HCO_3^- formed from the metabolic production and hydration of CO_2 within the cell (assuming that hydration of one mole of CO_2 generates one mole of HCO_3^-, residual intracellular HCO_3^- has been estimated at about 0·25 mM; Vanheel *et al.* 1984). Operation of the DIDS-sensitive Cl^-–HCO_3^- exchanger using metabolic HCO_3^- has been suggested previously for cardiac cells (Vanheel *et al.* 1984; Vaughan-Jones, 1986; Wu, Tsai & Tseng, 1994). This cannot, however, account for our putative CHE because the latter is DIDS *insensitive*. In addition, Vanheel *et al.* (1984) have pointed out that operation of Cl^-–HCO_3^- exchange using metabolic HCO_3^- would require up to 60% of all metabolically produced CO_2 being hydrated to HCO_3^- and utilized in transport rather than simply diffusing as CO_2 out of the cell, a situation which seems improbable, given the high CO_2 permeability of the sarcolemma. The basal rate of cellular CO_2 production is related to the basal rate of O_2 utilization, usually estimated at about 1 mM min^{-1} in cardiac cells (Piper, Probst, Schwartz, Hutter & Spiekermann, 1982; Howarth, Hunter, Berkoff & Moss, 1983). Assuming a respiratory coefficient of 0·8, this predicts a basal CO_2 production rate of 0·8 mM min^{-1}. The rate of operation of the novel Cl^--dependent acid loader (CHE) described in the present work is 0·5–1·0 mM min^{-1} at pH_o 6·40 (e.g. Fig. 10*A*) which is, again, similar to or even greater than the basal rate of CO_2 production. It therefore seems extremely unlikely that metabolic HCO_3^- generation can fuel the observed rates of operation of the novel CHE proposed in the present work. Moreover, in recent experiments (C. H. Leem & R. D. Vaughan-Jones, unpublished observations), we find that eliminating metabolic CO_2 production (Hepes-buffered conditions) by adding the aerobic inhibitors rotenone (10 μM) or cyanide (2 mM), fails to inhibit the fall of pH_i in low pH_o. This excludes directly a significant contribution of metabolic HCO_3^- to the functioning of CHE.

Pharmacological and ionic selectivity of dual acid-loading system. It is useful to summarize the evidence that the CHE carrier is distinct from the well-established Cl^-–HCO_3^- exchanger: (i) CHE works in the nominal absence of HCO_3^- and its rate is not significantly accelerated by the presence of HCO_3^- (see Fig. 10*B*); in other words anion selectivity for CHE would seem to be $OH^- \gg HCO_3^-$, whereas the same consideration for Cl^-–HCO_3^- exchange must be $HCO_3^- > OH^-$ on the grounds that DIDS-inhibitable acid loading is not evident in nominally HCO_3^--free conditions (it is recognized that OH^- or H^+ ion participation cannot be distinguished). (ii) CHE is DIDS insensitive, whereas previous work (Vaughan-Jones, 1982, 1986; Pucéat, Clement & Vassort, 1991; Xu & Spitzer 1994) has shown that cardiac Cl^-–HCO_3^- exchange (AE) is strongly inhibited by DIDS i.e. sensitivity to DIDS is AE $\gg$ CHE. It is therefore clear that, both pharmacologically and in terms of ionic selectivity, there must be two acid loaders in the guinea-pig cardiomyocyte. Although DBDS blocks CHE, it has also been reported to block AE (Poole & Halestrap, 1993) and so its use as a selective inhibitor of CHE in heart is probably not feasible.

Molecular biology of acid loaders. The AE-3 isoform has been proposed to represent the classical cardiac Cl^-–HCO_3^- exchanger (see Alper, 1991). Of particular interest is a recent report for two isoforms of the AE-3 protein in mammalian cardiac cells, including human (Yannoukakos, Stuart, Fernandez, Fey, Duyk & Alper, 1994). Pucéat and co-workers (Pucéat, Korichneva, Cassoly & Vassort, 1995) have also suggested the existence of two AE-type proteins in rat cardiomyocytes, but they suggest that only one is derived from AE-3, while the other is a truncated version of AE-1. We are intrigued that the presence of two or more anion exchange proteins in the cardiomyocyte may reflect our own evidence for more than one functional anion exchanger (AE and CHE). One of our carriers (CHE), however, is DIDS insensitive while at least the cardiac AE-3 isoforms identified by Yannoukakos *et al.* (1994) display the consensus amino acid sequence for DIDS binding.

Other paths for acid loading? A small, residual acid loading (about 15–20% of control loading) remains in Cl^--free solution (e.g. Figs 7 and 12). The cause of this is unknown. If it is a pathway that is also active under Cl^--containing conditions, it is likely to be voltage insensitive since total loading (in normal Cl_o^-) showed no sign of voltage sensitivity: the loading is therefore unlikely to be passive leakage of H^+ across the membrane. Our voltage-clamp data indicate that the sarcolemma is remarkably *tight* to protons (at least at the concentrations of protons encountered physiologically). This observation can be extended to include a lack of significant passive HCO_3^- flux through sarcolemmal anion channels, since it has been shown previously (Lagadic-Gossmann *et al.* 1992*b*) that pH_i is insensitive to large voltage jumps in the presence of a 5% CO_2–HCO_3^- buffer.

While residual levels of acid loading in low pH_o could be caused by intracellular metabolic reactions an alternative explanation for acid loading in Cl^--free solution could be low levels of activation of AE and CHE by the Cl^- substitutes (aspartate, gluconate and glucuronate). Although it is assumed that these relatively large anions do not readily bind to and activate the AE and CHE carriers, this need not preclude low levels of congener activity. Finally, we do not preclude other minor pathways for acid entry into the cardiac cell.

Model of pH_i control in the ventricular myocyte

In the diagram shown in Fig. 13 we incorporate the dual acid-loading system into an updated model for pH_i control in the cardiomyocyte. The model now shows symmetry in that acid extrusion is via a dual system relying on HCO_3^- and H^+ ion transport, while acid loading is also via a dual system, relying this time, on HCO_3^- and OH^- ions. The dual acid-extrusion mechanism is a Na^+-coupled system (like

many secondary active transport carriers), whereas both elements of the acid-loading system are *Na^+ independent but Cl^- coupled.*

Energy requirements for dual acid loading

Equilibrium thermodynamics. At present we assume that both elements of the dual acid loader are simple ion exchangers, with no energy supplied from continuous hydrolysis of ATP. Evidence in favour of this (at least in Hepes-buffered conditions) comes from the fact that metabolic inhibitors did not inhibit low-pH_o-induced acid loading in the cardiac cell (Fig. 4). The pH_i at thermodynamic equilibrium, for a simple CHE, exchanging 'n' OH^- ions for each Cl^- ion can be shown to be:

$$pH_i = pH_o + 1/n \log[Cl_i^-/Cl_o^-] + [(n-1)/2{\cdot}3n]\, EF/RT. \quad (1)$$

Where the OH^- ion concentrations have been expressed as equivalent pH values, Cl_i^- and Cl_o^- are the intracellular and extracellular Cl^- ion concentrations, respectively, E is the sarcolemmal membrane potential and R, T and F have their usual meanings. If $n = 1$, the carrier becomes electroneutral CHE, and eqn (1) simplifies to:

$$pH_i = pH_o + \log([Cl^-]_i/[Cl^-]_o). \quad (2)$$

Equation (2) is the same as that describing the equilibrium condition for electroneutral ($n = 1$) AE (i.e. $[HCO_3^-]_o/[HCO_3^-]_i = [Cl^-]_o/[Cl^-]_i$), assuming that the cell is an open system for CO_2, where P_{CO_2}, the solubility constant for CO_2 and apparent pK_a for CO_2–HCO_3^- are the same on both sides of the membrane, and where the relationship between P_{CO_2}, pH and HCO_3^- is at equilibrium.

Taking typical values for Cl_o^- (150 mM), Cl_i^- (30 mM) and pH_o (7·40), the predicted equilibrium pH_i is 6·70 for both AE and CHE with $n = 1$. Thus, such carriers would not be at equilibrium in a resting myocyte with a typical pH_i of 7·20. Both carriers would be energized to mediate OH^- ion and HCO_3^- ion efflux in exchange for Cl^- ion influx, i.e. under normal conditions of pH_i and pH_o, they would act as acid loaders. Reduction of pH_o to 6·40 would enhance the driving force for acid entry by about fourfold, and it is under these latter conditions that we see significant inward traffic of acid equivalents.

Stoichiometry of Cl^-–OH^- exchanger. Of the two acid loaders, the AE carrier protein is believed to mediate electroneutral one-for-one Cl^-–HCO_3^- exchange. In the case of the novel CHE, however, we have no direct evidence for its stoichiometry but the fact that its rate of operation, when stimulated at low pH_o, is unaffected by depolarizing voltage jumps of up to 140 mV suggests that the system is voltage insensitive which is at least consistent with an electroneutral carrier. Voltage insensitivity of a carrier's kinetics need not, however, preclude electrogenicity. For example, if the net charge-carrying step associated with an unequal exchange of Cl^- and OH^- ions during the carrier cycle were not rate limiting in the voltage range tested (and assuming the voltage range did not cross the electrogenic carrier's reversal potential; see eqn (1)), then no voltage sensitivity in the transport cycle need be evident.

Voltage-jump experiments, such as that shown in Fig. 6 can be used to place limits on the possible stoichiometry of CHE. The lack of voltage sensitivity of acid loading at pH_i

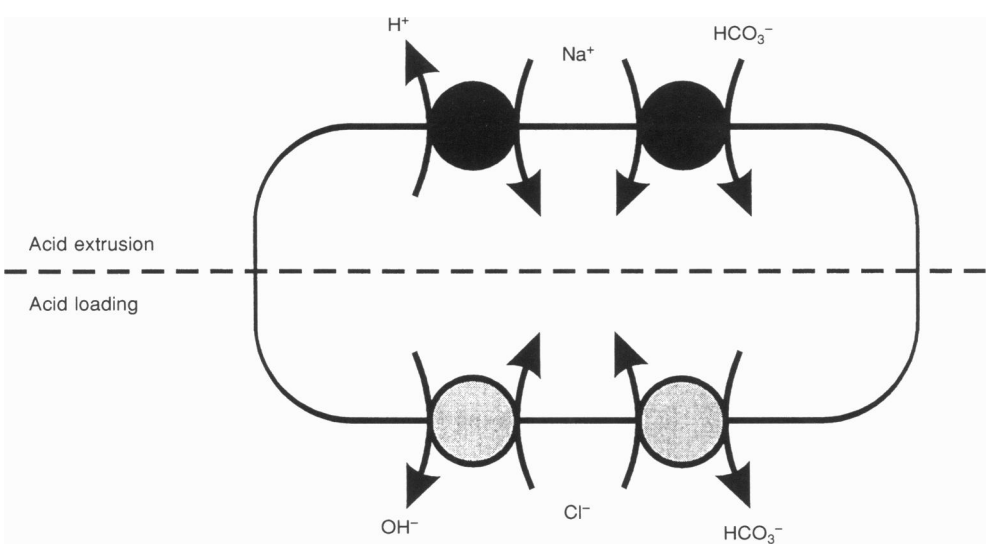

Figure 13. Model of pH_i control in the ventricular myocyte

The dual acid-extrusion system (Na^+–H^+ exchange and Na^+–HCO_3^- symport) is counterbalanced by a dual acid-loading system consisting of Cl^-–HCO_3^- exchange and the putative Cl^-–OH^- exchange (alternative configuration for this latter carrier is H^+–Cl^- co-influx).

7·00, pH_o 6·40 and ± 70 mV (Fig. 6) indicates that stoichiometry (n) must be $> n = 0·33$ and $< n = 3·0$. Coupling ratios outside these limits are excluded on the grounds that the voltage jumps would either neutralize or reverse the electrochemical driving force for net acid entry through the carrier (calculations based on eqn (1) above) thus either inhibiting or reversing net acid-equivalent flux across the cell membrane (an event which clearly did not occur). Even larger voltage jumps than those shown in Fig. 6 will be required to test for $n = 0·5$ (i.e. OH^-–$2Cl^-$) or $n = 2$ (i.e. $2OH^-$–Cl^-) as possible coupling ratios. It should be noted, however, that the coupling of $n = 1·0$, perhaps the most likely coupling value, also falls squarely within our range of possible n values, and net acid flux at this coupling ratio will display no true reversal potential (cf. eqn (2) above). In summary, while voltage insensitivity of acid loading is suggestive of an electroneutral CHE (or an electroneutral H^+–Cl^- co-transporter), we cannot rule out electrogenic ionic coupling ratios of, say, $2OH^-$–Cl^- or OH^-–$2Cl^-$. Larger ratios (e.g. $3OH^-$–Cl^- or OH^-–$3Cl^-$) can be excluded.

Dependence of pH_i on pH_o

The present work answers the question of how pH_i is influenced by a fall of pH_o. Figure 13 implies that pH_i is set by the balance between the activity of the acid extruders and acid loaders in the sarcolemma. An imbalance in the activity of these carriers will lead to a change of pH_i. In Hepes-buffered conditions, extracellular acidosis reduces NHE-mediated acid extrusion (extracellular pK_a (pK_o) for cardiac NHE is about 7·2, Vaughan-Jones & Wu, 1990) while simultaneously stimulating CHE-mediated acid influx. The pH_i will therefore fall. The fall stabilizes, presumably because intracellular acidosis reactivates H^+ extrusion on NHE and when this matches the CHE-mediated acid influx, the balance of acid fluxes across the membrane is restored. As indicated in Fig. 2*B*, NHE activity at this new balance point is *higher* than under control (pH_o 7·40) conditions because it is counteracting the enhanced acid influx on CHE. Thus, paradoxically, while tonic pH_o reduction initially inhibits NHE activity, in the steady-state NHE activity is stimulated.

A rise of pH_o back to 7·40 would be expected to reverse the above sequence of events leading to a return of pH_i to resting values, a process mediated by acid extrusion on NHE (recovery is amiloride blocked; see Fig. 2*A*) and assisted by the fact that acid loading on CHE is now reduced because of the high pH_o.

A similar sequence of events during extracellular acidosis presumably occurs in CO_2–HCO_3^--buffered conditions except that, at any pH_o, a balance among two extruders (NHE and Na^+–HCO_3^- symport) and two loaders (CHE and Cl^-–HCO_3^- exchange) must now be achieved. The magnitude of the fall of pH_i will therefore depend on the pH_o *versus* pH_i sensitivities of all the carriers. While intracellular *versus* extracellular pH sensitivity is well documented for NHE, it is less clearly defined for the other carriers. Consequently it is not yet possible to model quantitatively the magnitude of fall of pH_i with pH_o.

Acid loaders and intracellular alkali regulation

An important question is whether the dual acid-loading system is responsible for pH_i recovery from an intracellular *alkali* load, under conditions where pH_o remains at its normal level of 7·40. Such intracellular alkali regulation was first described in multicellular cardiac Purkinje fibres (Vaughan-Jones, 1982), where the AE carrier was clearly implicated. It remains to be determined, however, if the CHE carrier in the ventricular cell also plays a role under these circumstances. It is notable that, in nominally HCO_3^--free conditions, pH_i recovery from an intracellular alkali load is readily observed in the ventricular myocyte (see e.g. pH_i recovery from the alkalosis induced in Fig. 9*A* by removal of 5% CO_2–HCO_3^-).

Novel Cl^-–OH^- exchanger: comparison with other cells

Other cardiac cells. This is the first report of the CHE carrier in a cardiac myocyte. It is not known if CHE is expressed in other regions of the heart, or in cardiac cells from other species. There are, however, hints in the literature that CHE or some related carrier may be functional in the sheep heart, since reduction of pH_o in HCO_3^--free conditions, produces a prompt fall of pH_i in the sheep Purkinje fibre (Ellis & Thomas, 1976; Vaughan-Jones & Wu, 1990). As in the present work, the fall is too fast to be accounted for simply in terms of inhibition (by low pH_o) of NHE (Vaughan-Jones & Wu, 1990): there must simultaneously be a stimulation of acid influx. Provisional data gathered for rat isolated ventricular myocytes also indicates a DIDS-insensitive but DBDS-sensitive acid loading in low pH_o, CO_2–HCO_3^--free conditions, suggesting possible expression of CHE in rat heart (C. H. Leem & R. D. Vaughan-Jones, unpublished observations).

Non-cardiac cells. There have been previous proposals for the existence of Cl^-–OH^- exchange in cell membranes. These have been specifically for epithelial membranes, and are based solely on radiolabelled Cl^- flux studies in vesicles prepared from brush-border membranes of rabbit renal cortex (Shiuan & Weinstein, 1984) and rabbit ileum (Fan, Faust & Powell, 1983), and from apical membranes of rat distal colon (Rajendran & Binder, 1993). Interestingly, this last report suggests the co-existence of an AE and a CHE carrier, although there is no evidence for the effect of these carriers on pH_i. It is not clear if the CHE proposed in these previous papers bears any resemblance to that identified in the present work. For example, the CHE carrier proposed for rat distal colon is DIDS inhibitable, although its sensitivity to DIDS is less than that of the co-expressed AE. The CHE found in heart is, in contrast, DIDS insensitive.

Dual acid loading: a general principle?

The present work is the first demonstration of a dual acid-loading system playing a significant role in general pH_i

control. Although dual acid-*extrusion* systems using two parallel carriers in the plasmalemma are common, especially in non-epithelial cells, for pH_i regulation from intracellular acid loads (one of the two extruders being HCO_3^- dependent), previous work has so far revealed only a *single* type of carrier responsible for acid loading, and for pH_i regulation from intracellular alkali loads (invariably a HCO_3^--dependent carrier). It will be of interest, therefore, to see if CHE commonly compliments the established acid-loading mechanisms such as AE in non-cardiac cells. In particular, it will be intriguing to see if a general principle of dual acid loading in cells matches that established so far for dual acid extrusion.

Alper, S. L. (1991). The band 3-related anion exchanger (AE) gene family. *Annual Review of Physiology* **53**, 549–564.

Blank, P. S., Silverman, H. S., Chung, O. K., Hogue, B. A., Stern, M. D., Hansford, R. G., Lakatta, E. G., & Capogrossi, M. C. (1992). Cytosolic pH measurements in single cardiac myocytes using carboxy-seminaphthorhodafluor-1. *American Journal of Physiology* **263**, H276–284.

Bountra, C., Powell, T. & Vaughan-Jones, R. D. (1990). Comparison of intracellular pH transients in single ventricular myocytes and isolated ventricular muscle of guinea-pig. *Journal of Physiology* **424**, 343–365.

Bountra, C. & Vaughan-Jones, R. D. (1989). Effect of intracellular and extracellular pH on contraction in isolated, mammalian cardiac muscle. *Journal of Physiology* **418**, 163–187.

Desilets, M. & Baumgarten, C. M. (1986). K^+, Na^+, and Cl^- activities in ventricular myocytes isolated from rabbit heart. *American Journal of Physiology* **251**, C197–208.

Eisner, D. A., Kenning, N. A., O'Neill, S. C., Pocock, G., Richards, C. D. & Valdeolmillos, M. (1989). A novel method for absolute calibration of intracellular pH indicators. *Pflügers Archiv* **413**, 553–558.

Ellis, D. (1977). The effects of external cations and ouabain on the intracellular sodium activity of sheep heart Purkinje fibres. *Journal of Physiology* **273**, 211–240.

Ellis, D. & Thomas, R. C. (1976). Microelectrode measurement of the intracellular pH of mammalian heart cells. *Nature* **262**, 224–225.

Fan, C. C., Faust, R. G. & Powell, D. W. (1983). Coupled sodium-chloride transport by rabbit ileal brush-border membrane vesicles. *American Journal of Physiology* **244**, G375–385.

Howarth, R. A., Hunter, D. R., Berkoff, H. A. & Moss, R. L. (1983). Metabolic cost of the stimulated beating of isolated adult rat heart cells in suspension. *Circulation Research* **52**, 342–351.

Lagadic-Gossmann, D., Buckler, K. J. & Vaughan-Jones, R. D. (1992*a*). Role of bicarbonate in pH recovery from intracellular acidosis in the guinea-pig ventricular myocyte. *Journal of Physiology* **458**, 361–384.

Lagadic-Gossmann, D., Vaughan-Jones, R. D. & Buckler, K. J. (1992*b*). Adrenaline and extracellular ATP switch between two modes of acid extrusion in the guinea-pig ventricular myocyte. *Journal of Physiology* **458**, 385–407.

Leem, C. H. & Vaughan-Jones, R. D. (1995). Mechanism of low pH_o-induced fall of pH_i in isolated ventricular myocytes of guinea-pig. *Japanese Journal of Physiology* **45**, suppl. 2, S17.

Maldonado, H. M. & Cala, P. M. (1994). Labeling of the Amphiuma erythrocyte K^+/H^+ exchanger with H_2DIDS. *American Journal of Physiology* **267**, C1002–1012.

Orchard, C. H. & Kentish, J. C. (1990). Effects of changes of pH on the contractile function of cardiac muscle. *American Journal of Physiology* **258**, C967–981.

Piper, H. M., Probst, I., Schwartz, P., Hutter, F. J. & Spieckermann, P. G. (1982). Culturing of calcium stable adult cardiac myocytes. *Journal of Molecular and Cellular Cardiology* **14**, 397–412.

Poole, R. C. & Halestrap, A. P. (1993). Transport of lactate and other monocarboxylates across mammalian plasma membranes. *American Journal of Physiology* **264**, C761–782.

Pucéat, M., Clement, O. & Vassort, G. (1991). Extracellular MgATP activates the Cl^-/HCO_3^- exchanger in single rat cardiac cells. *Journal of Physiology* **444**, 241–256.

Pucéat, M., Korichneva, I., Cassoly, R. & Vassort, G. (1995). Identification of band 3-like proteins and Cl^-/HCO_3^- exchange in isolated cardiomyocytes. *Journal of Biological Chemistry* **270**, 1315–1322.

Rajendran, V. M. & Binder, H. J. (1993). Cl^--HCO_3^- and Cl^--OH^- exchanges mediate Cl^- uptake in apical membrane vesicles of rat distal colon. *American Journal of Physiology* **264**, G874–G879.

Richmond, P. & Vaughan-Jones, R. D. (1993). K^+–H^+ exchange in isolated carotid body type-1 cells of the neonatal rat is caused by nigericin contamination. *Journal of Physiology* **467**, 277*P*.

Shiuan, D. & Weinstein, S. W. (1984). Evidence for electroneutral chloride transport in rabbit renal cortical brush border membrane vesicles. *American Journal of Physiology* **247**, F837–847.

Sun, B. & Vaughan-Jones, R. D. (1994). Effect of extracellular pH on intracellular pH in isolated guinea-pig ventricular myocyte. *Journal of Physiology* **475.P**, 83*P*.

Thomas, R. C. & Meech, R. W. (1982). Hydrogen ion currents and intracellular pH in depolarized voltage-clamped snail neurones. *Nature* **299**, 826–828.

Vanheel, B. & de Hemptinne, A. (1985). Intracellular pH in depolarized cardiac Purkinje strands. *Pflügers Archiv* **405**, 118–126.

Vanheel, B., de Hemptinne, A. & Leusen, I. (1984). Analysis of Cl^--HCO_3^- exchange during recovery from intracellular acidosis in cardiac Purkinje strands. *American Journal of Physiology* **246**, C391–400.

Vaughan-Jones, R. D. (1979). Regulation of chloride in quiescent sheep-heart Purkinje fibres studied using intracellular chloride and pH-sensitive micro-electrodes. *Journal of Physiology* **295**, 111–137.

Vaughan-Jones, R. D. (1982). Chloride-bicarbonate exchange in the sheep cardiac purkinje fibre. In *Intracellular pH: Its Measurement, Regulation, and Utilization in Cellular Functions*, ed. Nuccitelli, R. & Deamer, D., pp. 239–252. Alan Liss, New York.

Vaughan-Jones, R. D. (1986). An investigation of chloride–bicarbonate exchange in the sheep cardiac Purkinje fibre. *Journal of Physiology* **379**, 377–406.

Vaughan-Jones, R. D. & Wu, M. L. (1990). Extracellular H^+ inactivation of Na^+–H^+ exchange in the sheep cardiac Purkinje fibre. *Journal of Physiology* **428**, 441–466.

Wu, M. L., Tsai, M. L. & Tseng, Y. Z. (1994). DIDS-sensitive pH_i regulation in single rat cardiac myocytes in nominally HCO_3^- free conditions. *Circulation Research* **75**, 123–132.

Xu, P. & Spitzer, K. W. (1994). Na^+-independent Cl^--HCO_3^- exchange mediates recovery of pH_i from alkalosis in guinea-pig ventricular myocytes. *American Journal of Physiology* **267**, H85–91.

Yannoukakos, D., Stuart Tilley, A., Fernandez, H. A., Fey, P., Duyk, G. & Alper, S. L. (1994). Molecular cloning, expression, and chromosomal localization of two isoforms of the AE3 anion exchanger from human heart. *Circulation Research* **75**, 603–614.

Zhao, J., Hogan, E. M., Bevensee, M. O. & Boron, W. F. (1995). Out-of-equilibrium CO_2/HCO_3^- solutions and their use in characterizing a new K^+/HCO_3^- cotransporter. *Nature* **374**, 636–639.

Acknowledgements

This work was funded by a grant (R.D.V.-J.) from the British Heart Foundation.

Author's present address

B. Sun: New England Medical Center, Molecular Cardiology Research Center, NEMC 80, 750 Washington Street, Boston, MA 02111, USA.

Author's email address

R. D. Vaughan-Jones: rdvj@physiol.ox.ac.uk

Received 7 November 1995; accepted 10 May 1996.